J. Biochem. **123**, 150-156 (1998)

Small-Angle X-Ray Scattering and Computer-Aided Molecular Modeling Studies of 20 kDa Fragment of Porcine Amelogenin: Does Amelogenin Adopt an Elongated Bundle Structure?[1]

Norio Matsushima,*,[2] Yoshinobu Izumi,† and Takaaki Aoba‡

**School of Health Sciences, Sapporo Medical University, Chuo-ku, Sapporo 060;* †*Graduate School of Engineering, Yamagata University, Yamagata 992; and* ‡*Department of Pathology, Faculty of Dentistry, Nippon Dentistry University, Chiyoda-ku, Tokyo 102*

Received for publication, August 19, 1997

Amelogenins, which are major matrix constituents in the developing tooth, play a regulatory role in the process of enamel crystal formation. Porcine amelogenin with 173 amino acid residues is rich in proline, glutamine, leucine, and histidine. We utilized the small-angle X-ray scattering (SAXS) technique to examine the solution structure of porcine amelogenin. Samples used were two porcine amelogenins with apparent molecular weights of 20 kDa (amino acids 1 to 148) and 13 kDa (amino acids 46 to 148) on SDS-PAGE. Prior to SAXS measurements, the protein samples were dissolved in 2% (v/v) acetic acid to give a concentration range up to 10 mg/ml. Comparison between *Rg* (the overall radius of gyration) and *Rc* (the cross-sectional radius of gyration) revealed that the 20 kDa amelogenin exists in this solution as asymmetric particles with a length of about 15 nm, presumably corresponding of dimers. Based on these experimental data and computer-aided molecular modeling studies, we propose that the 20 kDa amelogenin adopts an elongated bundle structure which mainly consists of extended structures similar to polyproline II and/or β-strand, interspersed with β-turn or loop.

Key words: elongated structure, modeling, porcine amelogenin, small-angle X-ray scattering.

Enamel of erupted teeth is the hardest tissue in the body. However, the forming enamel is soft in texture, being rich in organic matter and water. The amelogenins, *i.e.*, major constituents of the extracellular matrix in forming enamel, account for over 90% of the total proteins secreted by the ameloblasts during developmental stages (*1*). The amino acid sequences of the molecules from a number of mammalian species including pig have been determined (*2-13*). The analyses showed high contents of proline, glutamine, leucine, and histidine, and the presence of repeated sequences of -Pro-Xaa-Pro- or -Pro-Xaa-Xaa-Pro- (where Xaa is any amino acid) in the central domain of the proteins. Thus, the amelogenins have hydrophobic properties.

To date, many approaches using X-ray diffraction and ^{1}H-NMR have completely failed to determine the secondary or tertiary structure of amelogenins [for a review of amelogenin structure, see Fincham *et al.* (*14*)]. Based on studies using circular dichroism (CD), Fourier-transform infrared (FTIR) spectroscopy, and Raman spectroscopy, it was predicted that bovine amelogenin adopts β-sheet structures and β-turns (*15-18*). A recent CD study using porcine amelogenin and its fragments suggested that the structure of the whole protein consists of three discrete folding units (*15*). However, the folding pattern and tertiary structure of the amelogenins are still unknown.

In the present study, we used the small-angle X-ray scattering (SAXS) technique to explore the size and shape of amelogenin molecules in aqueous solution. The use of synchrotron orbital radiation as an intense X-ray source enabled us to collect experimental data within a reasonable time and without appreciable smearing effects. On the basis of the SAXS data obtained, and the results of computer-aided molecular modeling, a new structural model for porcine amelogenins is proposed.

MATERIALS AND METHODS

Sample Preparation—The secreted porcine amelogenin, which migrates to the position corresponding to 25 kDa on SDS-PAGE, consists of 173 amino acid residues (*2*). Its amino acid sequence is shown in Fig. 1. Shortly after secretion, this intact amelogenin is degraded enzymatically, giving rise to fragments which migrate to 20, 13, and 5 kDa on SDS-PAGE (*19, 20*). The 20 kDa fragment is sparingly soluble in neutral solutions and becomes a major component of the extracellular matrix during the maturation of enamel tissue (*21*). In contrast, the 13 kDa fragment

[1] This work has been performed with the approval of the Photon Factory Advisory Committee (Proposal No. 95G089).

[2] To whom correspondence should be addressed. Tel: +81-11-611-2111, Fax: +81-11-613-7134, E-mail: matusima @ shs.sapmed.ac.jp.

Abbreviations: SAXS, small-angle X-ray scattering; CD, circular dichroism; FTIR, Fourier transform infrared; *Rg*, overall radius of gyration; *Rc*, cross-sectional radius of gyration; SDS-PAGE, sodium dodecyl sulfate-polyacrylamide gel electrophoresis.

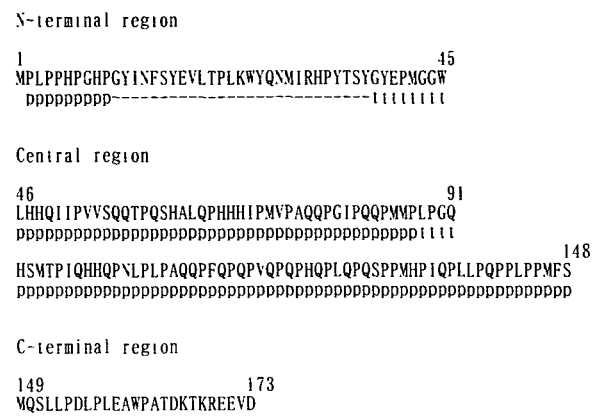

Fig. 1. **Amino acid sequence of porcine amelogenin reported by Yamakoshi *et al.* (*2*) and the secondary structure of its 20 kDa fragment (with amino acids 1 to 148) proposed here for modeling.** The polyproline II elements are indicated below the sequence with the letter "p"; β-strand are indicated with the symbol "-," and β-turn or loop with the letter "t."

is soluble and is concentrated in the fluid phase *in vivo* (*21*). The porcine amelogenin samples (20 and 13 kDa) that were used in the current work were well characterized by SDS-gel and Western blots using anti-porcine 20 kDa amelogenin, and by determination of their amino acid composition and partial sequences at both the N- and C-termini (*19-23*). The 20 kDa amelogenin comprises 148 amino acid residues and has the sequences Met-Pro-Leu- at the N-terminus and -Phe-Ser at the C-terminus (*21*). The 13 kDa fragment has Leu-His- and -Phe-Ser sequences at its N- and C-termini, corresponding to Leu46 to Ser148 (*21*). This preparation procedure was originally developed by Fukae *et al.* (*19*). Using porcine amelogenin samples collected by means of the same procedures, this group of investigators biochemically determined the whole amino acid sequence of 20 and 25 kDa porcine amelogenins (*2*). From studies using the purified 25 kDa porcine amelogenin as substrate, it was also verified that the protease isolated from secretory porcine enamel cleaves the amelogenin at specific sites, yielding the 20 and 13 kDa moieties (*24*). Although there remains controversy regarding phosphorylation of Ser16 of porcine amelogenins (*25, 37*), we have no positive evidence for phosphorylation in the 20 kDa amelogenin. SAXS measurement was done for these 20 and 13 kDa amelogenin fragments.

Small-Angle X-Ray Scattering—The measurements were performed using synchrotron orbital radiation with an instrument for SAXS installed at station BL-10C of the Photon Factory, Tsukuba. The X-ray beam line was equipped with a toroidal focusing mirror and a double crystal monochromator. The monochromatization was achieved by using silicon (111) reflection. The X-ray wavelength of 0.1488 nm was selected. Data were recorded using a one-dimensional position-sensitive proportional detector with a delay line readout. Corrections for the slit-smearing effect were not made, because quasi-type optics were used. The details of the optics and instrument were given elsewhere (*26*).

Prior to SAXS measurements, weighed amounts of the protein sample were dissolved in 2% (v/v) acetic acid and kept on ice. Under these conditions, the 20 and 13 kDa amelogenins were soluble enough to yield a maximum concentration of 10 mg/ml.

The sample solution was placed in a quartz cell of 70 μl in volume, and the temperature was kept at 5.0 ± 0.1°C by circulating water through the sample holder. The scale of the reciprocal parameter, Q, being equal to $(4\pi\sin\theta)/\lambda$, was calibrated by observation of the peaks from dried chicken collagen, where 2θ is the scattering angle and λ is the X-ray wavelength. Scattering data for Guinier plots were collected for 600 or 1,200 s at individual sample concentrations, since irradiation of the fragments for periods up to 1,200 s produced no change in the scattering profiles. The data were analyzed using a PC-9801RA personal computer (NEC).

Previous low-angle laser light scattering analysis showed that the 20 kDa amelogenin exists in a monomeric form at pH 5.3 and 25°C (*15*). The SAXS measurements were done in 2% (v/v) acetic acid (<pH 5.3) and 5°C. The possibility that the 20 kDa amelogenin exists in oligomeric form in this solution will be discussed later.

Scattering Data Analysis—Data analyses were done by Guinier methods. At small Q values, analyses of the scattering curves by the Guinier equation give the overall radius of gyration Rg (*27*):

$$\ln I = \ln I_o - Q^2Rg^2/3 \quad (1)$$

Here I_o is the scattered intensity at the reciprocal parameter $Q=0$ (at zero angle) and I is the scattered intensity at the reciprocal parameter, Q. The range of Q^2 (nm^{-2}) used for the Guinier plots was from the minima to 0.23, in which the minima of Q^2 were selected at various protein concentrations because of interparticle interference effects.

If one of the particle dimensions is much larger than the other two dimensions, the radius of gyration of the cross-section Rc is obtained in a larger Q range than that used in the Rg analyses (*28*):

$$\ln IQ = \ln (IQ)_o - Q^2Rc^2/2 \quad (2)$$

The cross-sectional analyses can be carried out for particles in which the ratio of the longest dimension to the other two dimensions is as low as 2:1, although at this limit the region of the scattering curve amenable to this analysis is restricted (*27*). Actually, the range of Q^2 (nm^{-2}) available for construction of the cross-sectional Guinier plots was from 0.39 to 3.6.

Computer-Aided Molecular Modeling—We attempted to construct a structural model of 20 kDa amelogenin having 148 amino acid residues on the basis of the Rg and Rc determined by the SAXS analyses as well as by taking into account the CD and FTIR spectral results obtained by other researchers (*15-18*). Computer-aided modeling was carried out using a Silicon Graphics interactive graphics system (INDIGO^2) with programs MMS (*29*) and SYBYL-6.3 (*30*). Energy minimization using the program running as part of SYBYL6.3 was also carried out to eliminate van der Waals clashes among all atomic positions. In order to validate the predicted structure of the 20 kDa amelogenin, the overall radius of gyration, Rg, was calculated by using the atomic coordinates obtained from the energy-minimized structure model according to the equation:

$$Rg^2 = \sum z_i R_i^2 / \sum z_i \quad (3)$$

where z_i is the atomic number for atom i and R_i is its

distance from the centroid of the atomic distribution in the molecule.

RESULTS

Small-Angle X-Ray Scattering—Figure 2 shows Guinier plots (*i.e.*, ln I *vs.* Q^2) for the 20 kDa fragment at protein concentrations ranging from 1.0 to 7.8 mg/ml in 2% (v/v) acetic acid. At lower concentrations, scattering X-ray intensities increased linearly in a low range of Q^2. *Rg* at certain protein concentrations can be calculated from the slope of this linear portion. However, at protein concentrations higher than 3.0 mg/ml, scattering X-ray intensities rapidly decreased at very small angles. This decrease in intensities is known to arise from interparticle interference effects and to become marked with increasing protein concentration (*27*). Such behavior could be prominent for particles adopting very asymmetric shapes at relatively low protein concentration (*31*). Figure 3 shows the overall radii of gyration, *Rg*s, calculated from the slope values, as a function of protein concentration. All resulting plots were linear in the concentration range from 1 to 4 mg/ml. Thus, we estimated the *Rg* value at zero concentration by extrapolation of the data obtained in the concentration range of 1.0 through 4.5 mg/ml. Finally, the obtained value of *Rg* at zero concentration was 4.36±0.10 nm (Table I).

The same approach was applied to the 13 kDa fragment. The estimation of *Rg* at zero concentration was not feasible for this fragment sample, because much weaker scattering intensities were obtained at protein concentrations lower

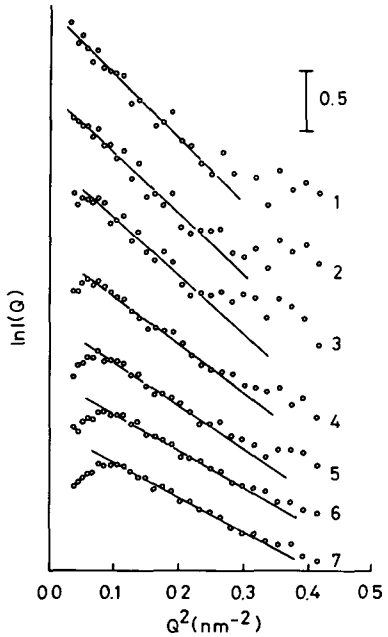

Fig. 2. **Guinier plots for the observed small angle scattering for 20 kDa fragment of porcine amelogenin at various protein concentrations.** Scattering curves in 2% (v/v) acetic acid. 1, 1.0 mg/ml; 2, 1.5 mg/ml; 3, 2.0 mg/ml; 4, 3.0 mg/ml; 5, 4.5 mg/ml; 6, 6.5 mg/ml; 7, 7.8 mg/ml.

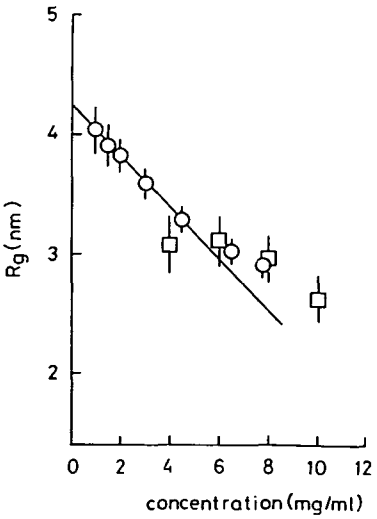

Fig. 3. **Protein concentration dependence of the overall radius of gyration, R_o, for two fragments of porcine amelogenin in 2% (v/v) acetic acid.** ○, 20 kDa fragment; □, 13 kDa fragment.

TABLE I. **Structural parameters of 20 and 13 kDa fragments of porcine amelogenin obtained by small angle X-ray scattering in 2% (v/v) acetic acid.** **L* and *d* are the length and diameter in a rod-like cylinder, respectively, and *a* and *b* are the semi-axes of a prolate ellipsoid, which approximate the asymmetric molecule.

	20 kDa fragment	13 kDa fragment
Rg (nm)	4.36±0.10	—
Rc (nm)	0.72±0.20	0.54±0.20
*L** (nm)	14.9±0.40	—
*d** (nm)	2.04±0.57	1.53±0.57
*a** (nm)	9.53±0.22	—
*b** (nm)	1.01±0.28	0.76±0.28

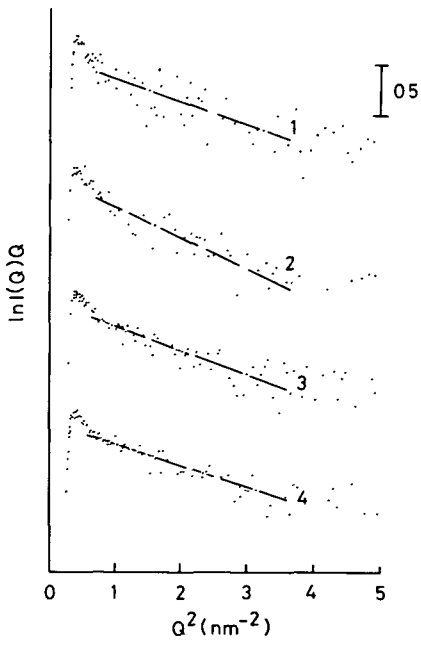

Fig. 4. **Cross-sectional plots of the observed small angle scattering for 20 kDa fragment of porcine amelogenin at protein concentrations.** Scattering curves in 2% (v/v) acetic acid. 1, 3.0 mg/ml; 2, 4.5 mg/ml; 3, 6.5 mg/ml; 4, 7.8 mg/ml.

than 4 mg/ml. Nevertheless, the *Rg*s at higher concentrations ranging from 6 to 10 mg/ml (in which interparticle interference effects appeared) were comparable with those obtained from the 20 kDa fragment in the corresponding concentration range.

Cross-sectional Guinier plots (*i.e.*, ln *IQ vs.* Q^2) used for determination of *Rc*s (the radii of the cross-sectional factor) are shown in Fig. 4 and the *Rc*s as a function of protein concentrations in Fig. 5. Scattering X-ray intensities were weaker and displayed greater deviation from the linear slopes. Despite such ambiguity, plots of *Rc vs.* protein concentration yielded linear relationships for both the 20 and 13 kDa fragments. The *Rc* of the 13 kDa fragment was smaller than that of the 20 kDa fragment, as shown in Table I.

Comparison of the observed *Rg* and *Rc* values clearly indicates that particles of the 20 kDa fragment are asymmetric in 2% (v/v) acetic acid. If the asymmetric particles are approximated by a rod-like cylinder or a prolate ellipsoid, knowledge of *Rg* and *Rc* gives the length *L* and diameter *d* of the rod-like cylinder and the semi-axes (*a* and *b*) of the prolate ellipsoid from the following equations (*27*).

Rod-like cylinder	$L^2 = 12(Rg^2 - Rc^2)$	(4a)
	$d^2 = 8Rc^2$	(4b)
Prolate ellipsoid	$a^2 = 5(Rg^2 - Rc^2)$	(5a)
	$b^2 = 2Rc^2$	(5b)

From Eqs. 4b and 5b, $d = 2b$. Structural parameters (*L*, *d*, *a*, and *b*) calculated according to these equations are shown in Table I.

Model—Previous CD studies of the 20 kDa fragment of porcine amelogenin showed a large negative peak at 203 nm at pH 5.3 (*15*), which is in agreement with the result for bovine amelogenin at pH 1.6 (*16*). The same peak was observed for the proline-rich sequence from the repeating unit of a giant secretory protein from *Chironomus tentans* (*32*). Such a spectral feature may be explained by the presence of polyproline II helix and β-turns (*32*). The FTIR spectra of bovine amelogenin also suggest the presence of polyproline II; it is possible to assign the observed amide I band at 1,636 cm^{-1} to not only β-sheet but also polyproline II (*33*). The amino acid sequence 1 to 10 is very rich in Pro (5 out of 10) and thus is reasonably assumed to adopt polyproline II structure. Also, the CD spectrum of the 45 amino acid residues at the N-terminal region showed a weak minimum around 215 nm, typical of β-strand conformation (*15*). Thus, we initially predicted the distribution of

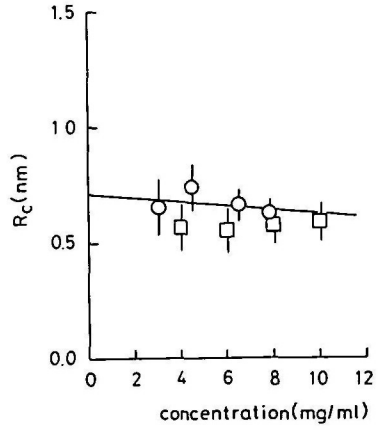

Fig. 5. **Protein concentration dependence of the radius of gyration of the cross section factor, *Rc*, for two fragments of porcine amelogenin in 2% (v/v) acetic acid.** ○, 20 kDa fragment; □, 13 kDa fragment.

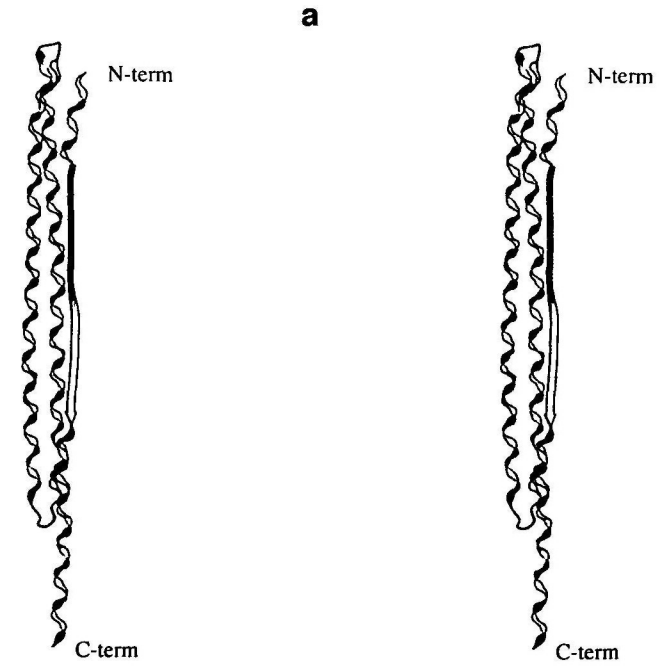

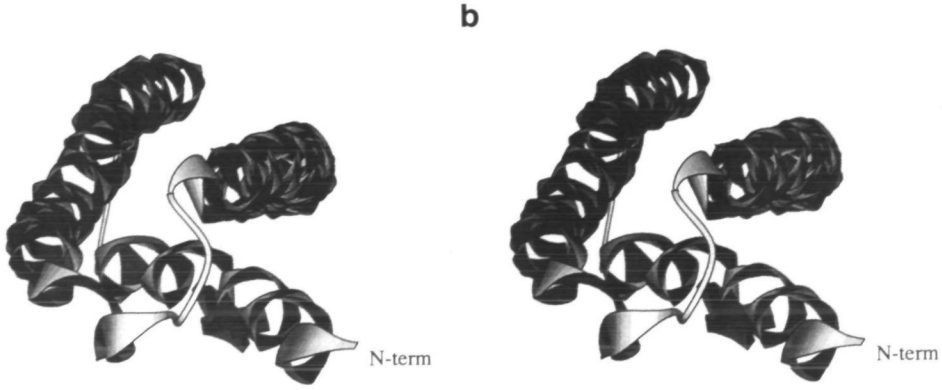

Fig. 6. **Ribbon representation of the modeled structure for 20 kDa fragment of porcine amelogenin (*43*).** The elongated model is characterized by a bundle structure. (a) The model viewed along the long axis; (b) the model viewed perpendicular to the long axis.

secondary structures in the target 20 kDa fragment as illustrated in Fig. 1. The pitches of β-strand and polyproline II are 0.35 and 0.29 nm, respectively (*34*). If the whole protein of the 20 kDa fragment adopts such secondary structures, the *Rg* of this very asymmetric rod-like molecule would correspond to 12.3-14.9 nm, but this would be three times larger than the X-ray experimental *Rg* value observed for the 20 kDa fragment. This consideration leads to the idea that the 20 kDa fragment is probably folded two times. In this connection, we paid attention to two characteristic sequences which are completely conserved within amelogenins from various species; one is rich in glycine at amino acids 38 to 45 (Gly-Tyr-Glu-Pro-Met-Gly-Gly-Trp), and the other is Pro-Gly at amino acids 89 to 90 (Fig. 1). The former seems to favor loop structure in proteins (*36*) and the latter strongly favors β-turn, especially type II turn (*35*). Using these preferences as a basis to construct a plausible tertiary structure of the 20 kDa fragment of porcine amelogenin, we started computer-aided structural modeling with the following parameters. The dihedral angles that define polyproline II are $\phi = -60°$, $\psi = +140°$, while the angles that define β-strand are $\phi = -119°$, $\psi = +120°$ (*34*). The Pro residues at amino acids 22 and 33 have $\phi = -60°$, $\psi = +120°$, because the permitted ϕ angle is only $\phi = -60 \pm 15°$. The dihedral angles of the remaining amino acids 38 to 45 and amino acids 88 to 91 were examined using some examples described by Efimov (*36*). Subsequently slight adjustments and energy minimization were made to optimize van der Waals contacts. All dihedral angles of the optimized structure were in allowed regions of the Ramachandran map (*34*).

The modeling results indicate that the predicted structure is characterized by an elongated bundle structure, as illustrated in Fig. 6, which may be regarded as a rod-like cylinder rather than a prolate ellipsoid. The predicted bundle structure consists of three parts of β-strand and/or polyproline II, interspersed with β-turn or loop. The predicted structure forms hydrophobic cores which might contribute to the structural stability; the first core consists of Leu3, Met85, Leu88, Met94, and Met95, the second core, Ile13, Phe15, Tyr17, Ile70, Val73, and Leu106, and the third core, Tyr34, Tyr37, and Ile50.

The atomic coordinates of the 20 kDa amelogenin model are available from the authors.

DISCUSSION

Elongated Bundle Structure—It has been well documented that amelogenin conformation is sensitive to variations in temperature, protein concentration, solution pH and ionic strength. The present SAXS studies indicated that the *Rg* values of the 20 kDa fragment linearly decrease with increasing protein concentration in the concentration range of 1 to 4 mg/ml (Fig. 3). This behavior is generally observed for many proteins in solution (*27*). We consider that no substantial change occurred in protein conformation within the concentration range studied, or, if it did, its magnitude was too small to have a major effect on the size and shape of the 20 kDa sample in solution.

The present SAXS studies provided evidence that particles of the 20 kDa fragment are highly asymmetric in 2% (v/v) acetic acid at 5°C. This conclusion is consistent with the well-known SDS-PAGE and molecular sieve data, showing that amelogenins do not behave like a globular protein in solution (*37*). The partial specific volume (ν_c) of amelogenin protein was reported to be 0.74 ml/g (*30*), so that the radius of gyration (*Rg*) for 20 kDa amelogenin in globular form is predicted to be 1.4 nm which is much smaller than the X-ray experimental values, as expected. This simple calculation also supports the bundle structure of the 20 kDa fragment. On the basis of the atomic coordinates of the proposed bundle structure, we calculated the *Rg* of the 20 kDa fragment according to Eq. 3. The calculated value of *Rg* (=4.32 nm) was compatible with the X-ray experimental *Rg* (=4.36 nm).

It is of interest to note that several proteins having a series of tandem repeats adopt unique protein folds, as described here for amelogenin. SAXS analysis indicated that α-zeins can be approximated by a nonglobular, prism-like shape (*38*). High-molecular-weight glutenin was observed to have a rod-like structure consisting of a novel supersecondary structure called polyproline, β-turn helix (*31*). X-ray crystal structure analysis showed that porcine ribonuclease inhibitor containing leucine-rich repeats takes a nonglobular, horseshoe shape (*39*). In the case of repeats of -Pro-Xaa-Pro- or -Pro-Xaa-Xaa-Pro- in the amelogenin, polyproline II structure was tentatively assigned. This structural components might contribute to the formation of the elongated bundle structure, but not the triple helix seen in collagen, which is characterized by tandem repeats of Gly-Xaa-Xaa.

Aggregation Properties—The aggregation properties of amelogenin are dependent on protein concentration, temperature, *etc.* (*40-42*). Recently dynamic light scattering, transmission electron and atomic force microscopy studies showed that the murine amelogenin with 179 amino acids forms a monodispersed aggregate structure with hydrodynamic radii ranging from 15 to 19 nm, at pH 7.8-8.0, ionic length 0.02-0.05 M, and protein concentration 0.5-2 mg/ml (*41, 42*). On the other hand, low-angle laser light scattering analysis showed that the 20 kDa amelogenin exists in a monomeric form at pH 5.3 and 25°C (*15*). The solution of 2% (v/v) acetic acid used here gives a value close to pH 5.3, rather than pH 7.8-8.0. In order to clarify whether the amelogenin molecules exist as a monomer or oligomers, we calculated the molecular weight (M_r) of the 20 kDa fragment in 2% (v/v) acetic acid at 5°C studied here according to the equation:

$$M_r = (NaV)/\nu_c \quad (6)$$

where *Na* is Avogadro's number, *V* the volume of a molecule, and $\nu_c = 0.74$ ml/g (*37*). We assumed that the amelogenin molecules have a rod-like cylinder [$V = \pi(d/2)^2 L$] or a prolate ellipsoid [$V = (4\pi/3)ab^2$] shape. The values of *d, L, a,* and *b* were obtained from the *Rg* and *Rc* values as described above. The results showed that in either case the calculated M_r for the 20 kDa amelogenin is about two times larger than the value for the monomeric molecule. Thus the protein may exist as a dimer at most in 2% (v/v) acetic acid. This does not rule out the possibility that some or most of the protein molecules exist in a monomeric form in the acetic solution because *Rc* or *d/b* values are less reliable than the *Rg* or *L/a* values. One also may suppose that there is an equilibrium between the monomer and dimer, so that the Guinier analysis gives the *z*-averaged *Rg* and *Rc* (*44*).

Concerning the presumed formation of dimers, it is feasible that a pair of the elongated monomers face each other parallel to their long axes. A stacking of the monomers aligning parallel to the long axis leads to dimerization. An important consideration is that the *Rg* value may not be affected substantially by the dimerization, because the length L of a rod-like cylinder or the longest dimension a of a prolate ellipsoid contributes predominantly to *Rg* according to Eqs. 4a and 5a. In fact, the *Rg* value predicted on the basis of the proposed dimer model is only 3 to 4% larger than that the *Rg* (=4.32 nm) calculated from the monomer model, indicating that the X-ray experimental *Rg* (=4.36 nm) is comparable to the calculated values irrespective of monomer or dimer structure.

Different aggregation behavior in various solutions and conditions has been observed for hydrophobic α-zeins and high-molecular-weight wheat glutenin, as well as amelogenin (*31, 38*). We think that such a property is a fundamental feature of hydrophobic proteins. The relevance of the elongated bundle structure of 20 kDa amelogenin obtained at 5°C and pH around 5 to the *in vivo* situation might be questioned. However, it is possible to imagine that, under different conditions, amelogenins retaining the characteristic elongated structure may lead to larger spheric aggregates as observed by Moradian-Oldak *et al.* (*41*) and Fincham *et al.* (*42*).

CONCLUSION

The SAXS studies indicated that the 20 kDa fragment of porcine amelogenins has an asymmetric shape with a length of about 15 nm in 2% (v/v) acetic acid at 5°C. We propose that amelogenin adopts an elongated bundle structure, which mainly consists of extended structures similar to polyproline II and/or β-strand, interspersed with β-turn or loop. The predicted structure appears to have a unique protein fold, which is different from the collagen triple helix or four-α-helix bundle. We would like to emphasize that the combination of computer-aided molecular modeling with small-angle X-ray scattering provides a useful method to examine the solution structure of molecules.

We are grateful to Mrs. H. Takezawa of Yamagata University for dedicated technical assistance in the scattering experiment and to Prof. K. Kobayashi and other members of the Photon Factory for their help in the scattering experiments at the Photon Factory. We also thank H. Konno for her help in preparing the manuscript.

REFERENCES

1. Termine, J.D., Belcourt, A.B., Christner, P.J., Conn, K.M., and Nylen, M.V. (1980) Properties of dissociatively extracted fetal tooth matrix proteins. I. Principal molecular species in developing bovine enamel. *J. Biol. Chem.* **255**, 9760-9768
2. Yamakoshi, Y., Tanabe, T., Fukae, M., and Shimizu, M. (1994) Porcine amelogenins. *Calcif. Tissue Int.* **54**, 69-75
3. Fincham, A.G. and Moradian-Oldak, J. (1993) Amelogenin post-translational modifications: carboxy-terminal processing and the phosphorylation of bovine and porcine "TRAP" and "LRAP" amelogenins. *Biochem. Biophys. Res. Commun.* **197**, 248-255
4. Snead, M.L., Lau, E.C., Zeichner-David, M., Fincham, A.G., Woo, S.L., and Slavkin, H.C. (1985) DNA sequence for cloned cDNA for murine amelogenin reveal the amino acid sequence for enamel-specific protein. *Biochem. Biophys. Res. Commun.* **129**, 812-818
5. Lau, E.C., Simmer, J.P., Bringas, Jr, P., Hsu, D.D.J., Hu, C.-C., Zeichner-David, M., Thiemann, F., Snead, M.L., Slavkin, H.C., and Fincham, A.G. (1992) Alternative splicing of the mouse amelogenin primary RNA transcript contributes to amelogenin heterogeneity. *Biochem. Biophys. Res. Commun.* **188**, 1253-1260
6. Shimokawa, H., Ogata, Y., Sasaki, S., Sobel, M.E., Mcquillan, C.I., Termine, J.D. and Young, M.F. (1987) Molecular cloning of bovine amelogenin cDNA. *Adv. Dent. Res.* **1**, 293-297
7. Gibson, C., Golub, E., Herold, R., Risser, M., Ding, W., Shimokawa, H., Young, M., Termine, J.D., and Rosenbloom, J. (1991) Structure and expression of the bovine amelogenin gene. *Biochemistry* **30**, 1075-1079
8. Takagi, T., Suzuki, M., Baba, T., Minegishi, K., and Sasaki, S. (1984) Complete amino acid sequence of amelogenin in developing bovine enamel. *Biochem. Biophys. Res. Commun.* **121**, 592-597
9. Nakahori, Y., Takenaka, O., and Nakagome, Y. (1991) A human X-Y homologous region encodes amelogenin. *Genomics* **9**, 264-269
10. Salido, E.C., Yen, P.H., Koprivnikar, K., Yu, L.C., and Shapiro, L.J. (1992) The human enamel protein gene amelogenin is expressed from both the X and the Y chromosomes [see comments]. *Am. J. Human Genet.* **50**, 303-316
11. Fincham, A.G., Hu, Y., Pavlova, Z., Slavkin, H.C., and Snead, M.L. (1989) Human amelogenins: sequences of "TRAP" molecules. *Calcif. Tissue Int.* **45**, 243-250
12. Bonass, W.A., Robinson, P.A., Kirkham, J., Shore, R.C., and Robinson, C. (1994) Molecular cloning and DNA sequence of rat amelogenin and a comparative analysis of mammalian amelogenin protein sequence divergence. *Biochem. Biophys. Res. Commun.* **198**, 755-763
13. Hu, C.C., Zhang, C., Qian, Q., Ryu, H., Moradian-Oldak, J., Fincham, A.G., and Simmer, J.P. (1996) Cloning, DNA sequence, and alternative splicing of opossum amelogenin mRNAs. *J. Dent. Res.* **75**, 1735-1741
14. Fincham, A.G., Lau, E.C., Simmer, J.P., and Zeichner-David, M. (1992) in *Chemistry and Biology of Mineralized Tissues* (Slavkin, H.C. and Price, P., eds.) pp. 187-201, Elsevier Science Publishers, Amsterdam
15. Goto, Y., Kogure, E., Takagi, T., Aimoto, S., and Aoba, T. (1993) Molecular conformation of porcine amelogenin in solution: three folding units at the N-terminal, central, and C-terminal regions. *J. Biochem.* **113**, 55-60
16. Renugopalakrishnan, V., Strawich, E., Morowitz, P.M., and Glimcher, M.J. (1986) Studies of the secondary structures of amelogenin from bovine tooth enamel. *Biochemistry* **25**, 4879-4887
17. Renugopalakrishnan, V., Pattabraman, N., Prabhakaran, M., Strawich, E., and Glimcher, M.J. (1989) Tooth enamel protein, amelogenin, has a probable beta-spiral internal channel, Gln112-Leu138, within a single polypeptide chain: preliminary molecular mechanics and dynamics studies. *Biopolymers* **28**, 297-303
18. Zheng, S., Tu, A.T., Renugopalakrishnan, V., Strawich, E., and Glimcher, M.J. (1987) A mixed beta-turn and beta-sheet structure for bovine tooth enamel amelogenin: Raman spectroscopic evidence. *Biopolymers* **26**, 1809-1813
19. Fukae, M., Ijiri, H., Tanabe, T., and Shimizu, M. (1979) Partial amino acid sequences of two proteins in developing porcine enamel. *J. Dent. Res.* **58**, 1000-1001
20. Shimizu, M. and Fukae, M. (1983) in *Mechanisms of Tooth Enamel Formation* (Suga, S., ed.) pp. 125-141, Quintessence Publ., Tokyo
21. Aoba, T., Tanabe, T., and Moreno, E.C. (1987) Proteins in the enamel fluid of immature porcine teeth. *J. Dent. Res.* **66**, 1721-1726
22. Aoba, T., Shimoda, S., Shimokawa, H., and Inage, T. (1992) Common epitopes of mammalian amelogenins at the C-terminus and possible functional roles of the corresponding domain in enamel mineralization. *Calcif. Tissue Res.* **51**, 85-91
23. Aoba, T., Shimoda, S., Akita, H., Holmberg, C., and Taubman, M.A. (1992) Anti-peptide antibodies reactive with epitopic domains of porcine amelogenins at the C-terminus. *Arch. Oral*

Biol. **37**, 249-255
24. Tanabe, T., Fukae, M., and Shimizu, M. (1994) Degradation of enamelins by proteinases found in porcine secretory enamel in vitro. *Arch. Oral Biol.* **39**, 277-281
25. Fincham, A.G., Moradian-Oldak, J., and Sarte, P.E. (1994) Mass-spectrographic analysis of a porcine amelogenin identifies a single phosphorylated locus. *Calcif. Tissue Int.* **55**, 398-400
26. Ueki, T., Hiragi, Y., Izumi, Y., Tagawa, H., Kataoka, M., Muroga, Y., Matsushita, T., and Amemiya, Y. (1983) KEK Progress Reports 83-1, Photon Activity Report, 1982/1983, VI-70-VI-71
27. Glatter, O. (1982) Data treatment in *Small Angle X-Ray Scattering* (Glatter, O. and Kratky, O., eds.) pp. 119-196, Academic Press, London
28. Pilz, I. (1982) Proteins in *Small Angle X-Ray Scattering* (Glatter, O. and Kratky, O., eds.) pp. 239-293, Academic Press, London
29. Dempsey, S. (1987) *Molecular Modeling System* (*MMS*), Department of Chemistry Computer Facility, Univ. of California at San Diego
30. Tripos (1996) SYBYL6.3, Tripos Associates, St. Louis, MO
31. Matsushima, N., Danno, G., Sasaki, N., and Izumi, Y. (1992) Small-angle X-ray scattering study by synchrotron orbital radiation reveals that high molecular weight subunit of glutenin is a very anisotropic molecule. *Biochem. Biophys. Res. Commun.* **186**, 1057-1064
32. Wellman, S.E., Hamodrakas, S.J., Kamitsos, E.I., and Case, S.T. (1992) Secondary structure of synthetic peptides derived from the repeating unit of a giant secretory protein from Chironomus tentans. *Biochim. Biophys. Acta* **1121**, 279-285
33. Suzuki, S., Ishiwata, Y., Shimanouchi, T., and Tsuboi, M. (1966) Infrared spectra of isotopic polyglycines. *Biopolymers* **4**, 337-350
34. Schultz, G.E. and Schirmer, R.H. (1979) in *Principles of Protein Structure*, pp. 66-107, Springer-Verlag, Berlin
35. Wilmot, C.M. and Thornton, J.M. (1988) Analysis and prediction of the different types of beta-turn in proteins. *J. Mol. Biol.* **203**, 221-232
36. Efimov, A.V. (1993) Standard structures in proteins. *Prog. Biophys. Mol. Biol.* **60**, 201-239
37. Strawich, E., Poon, P.H., Renugopalakrishnan, V., and Glimcher, M.J. (1985) Relative molecular mass determination of a major, highest relative molecular mass extracellular amelogenin of developing bovine enamel. *FEBS Lett.* **184**, 188-192
38. Matsushima, N., Danno, G., Takezawa, H., and Izumi, Y. (1997) Three-dimensional structure of maize α-zein proteins studied by small-angle X-ray scattering. *Biochim. Biophys. Acta* **1339**, 14-22
39. Kobe, B. and Deisenhofer, J. (1993) Crystal structure of porcine ribonuclease inhibitor, a protein with leucine-rich repeats. *Nature* **366**, 751-756
40. Nikiforuk, G. and Simmons, N.S. (1965) Purification and properties of protein from embryonic bovine enamel. *J. Dent. Res.* **44**, Suppl: 1119-1122
41. Moradian-Oldak, J., Simmer, J.P., Lau, E.C., Sarte, P.E., Slavkin, H.C., and Fincham, A.G. (1994) Detection of monodisperse aggregates of a recombinant amelogenin by l dynamic light scattering. *Biopolymers* **34**, 1339-1347
42. Fincham, A.G., Moradian-Oldak, J., Diekwisch, T.G.H., Lyaruu, D.M., Wright, J.T., Bringas, Jr. P., and Slavkin, H.C. (1995) Evidence for amelogenin "nanospheres" as functional components of secretory-stage enamel matrix. *J. Struct. Biol.* **115**, 50-59
43. Kraulis, P.J. (1991) MOLSCRIPT: a program to produce both detailed and schematic plots of protein structures. *J. Appl. Cryst.* **24**, 946-950
44. Guinier, A. and Fournet, G. (1955) in *Small-Angle Scattering of X-Rays*, p. 19, pp. 24-28, and pp. 135-136, Johns Wiley and Sons, New York